

# Valley Splitting Theory of SiGe/Si/SiGe Quantum Wells

Mark Friesen<sup>1,\*</sup>, Sucismita Chutia<sup>1</sup>, Charles Tahan<sup>2</sup>, and S. N. Coppersmith<sup>1</sup>  
<sup>1</sup>*Department of Physics, University of Wisconsin-Madison, Wisconsin 53706, USA and*  
<sup>2</sup>*Cavendish Laboratory, University of Cambridge,*  
*JJ Thomson Ave, Cambridge CB3 0HE, United Kingdom*

We present an effective mass theory for SiGe/Si/SiGe quantum wells, with an emphasis on calculating the valley splitting. The theory introduces a valley coupling parameter,  $v_v$ , which encapsulates the physics of the quantum well interface. The new effective mass parameter is computed by means of a tight binding theory. The resulting formalism provides rather simple analytical results for several geometries of interest, including a finite square well, a quantum well in an electric field, and a modulation doped two-dimensional electron gas. Of particular importance is the problem of a quantum well in a magnetic field, grown on a miscut substrate. The latter may pose a numerical challenge for atomistic techniques like tight-binding, because of its two-dimensional nature. In the effective mass theory, however, the results are straightforward and analytical. We compare our effective mass results with those of the tight binding theory, obtaining excellent agreement.

PACS numbers: 73.21.Fg, 73.20.-r, 78.67.De, 81.05.Cy

## I. INTRODUCTION

Silicon heterostructures form the basis of numerous semiconductor technologies. To understand future silicon heterostructure devices that involve quantum effects, one must consider the quantum states associated with the degenerate valleys in the conduction band structure. In a strained quantum well, the valley degeneracy is two-fold. This degeneracy is lifted by the singular nature of the quantum well interface, with characteristic energy splittings of order 0.1-1 meV for the case of SiGe/Si/SiGe quantum wells.<sup>1,2,3,4,5,6</sup> Because this splitting is comparable in size to the Zeeman splitting, the valley states can compete with spin states for prominence in quantum devices.<sup>7</sup> For emerging technologies like silicon spintronics<sup>8,9,10,11,12</sup> and quantum computing,<sup>13,14,15,16</sup> it is therefore crucial to obtain a solid physical understanding of the valley physics, and to develop a predictive theory for the valley states.

The technological significance of valley states was recognized long before the current interest in quantum devices.<sup>17,18</sup> Early studies focused on bulk silicon, particularly on the electronic states of shallow donors. In this case, valley splitting was known to originate from the singular core of the donor potential, known as the “central cell.”<sup>19</sup> In one theoretical approach, the many-body interactions associated with the central cell were projected onto a single-electron, effective mass (EM) framework, allowing the energy spectrum of the low-lying hydrogenic states to be computed from first principles.<sup>20,21</sup> Reasonable agreement with experiments was attained. However, because of the complicated projection procedure, a general purpose EM theory was not obtained until more recently.<sup>22</sup>

Related techniques were applied to the problem of valley splitting in a semiconductor heterostructure. There were several attempts to develop an EM theory, which is well suited for treating inhomogeneous conditions, including conduction band offsets and non-uniform elec-

tric fields associated with modulation doping and top-gates. However, the resulting theories proved controversial, and many important valley splitting problems remain unsolved.

Atomistic approaches like tight-binding (TB) theory have recently emerged as important tools for calculating the valley splitting.<sup>23</sup> These techniques have been applied to a range of heterostructure geometries,<sup>23,24,25</sup> providing crucial insights and predictions for experiments that that may be difficult to implement. For example, the valley splitting has been predicted to oscillate as a function of the quantum well width.<sup>23</sup> These oscillations can be reduced, or even eliminated, by applying an electric field.

Here, we develop an EM formalism, which corroborates the atomistic results quite accurately, and which provides a simple physical explanation for the intriguing oscillations. Specifically, we show that the behavior occurs because of valley coupling interference between the top and bottom interfaces of the quantum well. In an electric field, the wavefunction is squeezed to one side of the quantum well, thereby eliminating the interference effect. We also use the EM theory to move beyond simple one-dimensional (1D) geometries. For example, quantum wells grown on a miscut substrate represent an inherently 2D problem. Here, we show that interference effects also play a crucial role for such miscut geometries, causing a strong suppression of the valley splitting at low magnetic fields.

The paper is organized as follows. In Sec. II, we review the two predominant approaches to valley coupling. In Sec. III, we describe an extension to the conventional effective mass theory that provides a perturbative scheme to incorporate valley coupling. In Sec. IV, we use a tight binding theory to calculate the new input parameter for the EM theory – the valley coupling  $v_v$  – as a function of the conduction band offset  $\Delta E_c$ . In Sec. V, we apply the EM theory to a finite square well geometry. In Sec. VI, we obtain an analytical solution for a quantum well in an external electric field. In Sec. VII, we consider the

experimentally important problem of a two-dimensional electron gas (2DEG). In Sec. VIII, we study the valley splitting in a magnetic field, when the quantum well is misaligned with respect to the crystallographic axes. Finally, in Sec. IX, we summarize our results and conclude.

## II. EFFECTIVE MASS APPROACH

Earlier EM approaches for the valley splitting in a heterostructure include the “electric breakthrough” theory of Ohkawa and Uemura,<sup>26,27,28</sup> and the surface scattering theory of Sham and Nakayama.<sup>29</sup> A review of these theories and other related work is given in Ref. [18]. The Ohkawa-Uemura formalism leads to a multi-valley EM theory based on a two-band model involving the lowest two conduction bands at the  $\Gamma$  point of the Brillouin zone,  $|\Gamma_1(S)\rangle$  and  $|\Gamma_{15}(Z)\rangle$ .<sup>30</sup> The resulting bulk dispersion relation has a local maximum at the  $\Gamma$  point, and it exhibits two degenerate valleys, at roughly the correct positions in  $k$ -space. The sharp confinement potential at the heterostructure interface produces a natural coupling between the two  $z$  valleys. For an infinite square well of width  $L$ , the Ohkawa-Uemura theory obtains a valley splitting of the form  $E_v \sim \sin(2k_0L)/L^3$ , where  $k_0\hat{z}$  is the location of the valley minimum in the Brillouin zone.<sup>28</sup> This result was later confirmed by TB theory.<sup>23,24</sup> The theory therefore captures the main qualitative aspects of the valley physics, with no additional input parameters besides those describing the bulk dispersion relation. In this sense, it is a first principles theory of valley splitting.

However, some aspects of the Ohkawa-Uemura theory have been called into question. First, it has been criticized for its inaccurate description of the dispersion relation near the bottom of the valleys,<sup>18</sup> leading to quantitative errors. More importantly, the method relies on a closed EM description, which cannot easily incorporate microscopic details of the quantum well barrier. This contradicts the fact that the valley coupling arises from physics occurring within several angstroms of the interface.<sup>29</sup> Such distances are much smaller than any EM length scale, and cannot be accurately described within any EM theory.

A physically appealing description of the heterostructure interface has been put forward by Sham and Nakayama. These authors develop a theory in which the reflection, transmission, and valley-scattering of waves at a Si/SiO<sub>2</sub> interface is built directly into the Bloch function basis states. Since the confinement is incorporated into the basis set, it does not also appear as an external potential in the envelope equation. Any additional potentials entering envelope equation (*e.g.*, electrostatic potentials) are therefore smooth, and easily accommodated in an EM approach. The analytical results for the valley splitting are similar to Ohkawa-Uemura. Indeed, the two approaches have been shown to be closely related.<sup>31</sup>

The Sham-Nakayama theory has also been criticized. First, the theory is not self-contained – a single input pa-

rameter  $\alpha$  is introduced to characterize the microscopic width of the interface. Although Sham and Nakayama provide an estimate for  $\alpha$ , the parameter is phenomenological. More importantly, the resulting EM theory is somewhat cumbersome, and cannot provide simple analytical solutions for the heterostructure geometries considered here.

In this paper, we develop an EM theory which retains the desirable qualities of both the Ohkawa-Uemura and Sham-Nakayama approaches. We introduce a valley coupling parameter  $v_v$ , which efficiently describes the valley coupling for any type of interface, and which enables simple analytical results for the valley splitting that are in agreement with atomistic theories.

## III. EFFECTIVE MASS THEORY

The EM theory of Kohn and Luttinger<sup>17</sup> provides an excellent description of electrons in a semiconductor matrix under the influence of a slowly varying confinement potential  $V(\mathbf{r})$ .<sup>32</sup> Here, “slowly” is defined with respect to the crystalline unit cell of length  $a$ :

$$V(\mathbf{r})/|\nabla V(\mathbf{r})| \gg a. \quad (1)$$

In practice, the EM approach is extremely robust, often proving accurate well outside its range of validity. Indeed, the standard textbook descriptions of shallow donors and quantum wells are both based on an EM theory,<sup>32</sup> despite the singular nature of their confinement potentials.

When the validity criterion (1) is not satisfied, it is a good idea to compare the EM results with microscopic or atomistic approaches, such as the TB theory of Sec. IV. For GaAs quantum wells, the EM theory provides quantitatively accurate results in most situations. The approach only breaks down for very narrow quantum wells, or for high subband indices.<sup>33</sup> On the other hand, for indirect gap semiconductors like silicon, the EM theory must be extended if valley splitting becomes an important issue. A singular confinement potential causes valley coupling, and calls for a more sophisticated treatment. Here, we provide a discussion of both the general multi-valley EM approach, and of the valley coupling, which arises from a sharp quantum barrier.

In the standard EM theory, the wavefunction for a conduction electron in bulk Si can be written as a sum of contributions from the six degenerate valleys. However, the lattice mismatch between Si and Ge in a Si<sub>1-x</sub>Ge<sub>x</sub>/Si/Si<sub>1-x</sub>Ge<sub>x</sub> quantum well causes tensile strain in the Si layer (assuming strain-relaxed SiGe). As a result, four of the six valleys rise in energy, while the two  $z$  valleys fall in energy.<sup>34</sup> The strain splitting is on the order of 200 meV for the composition corresponding to  $x = 0.3$ .<sup>35</sup> Consequently, only  $z$  valleys play a role in typical low-temperature experiments.

The EM wavefunction for strained silicon can then be

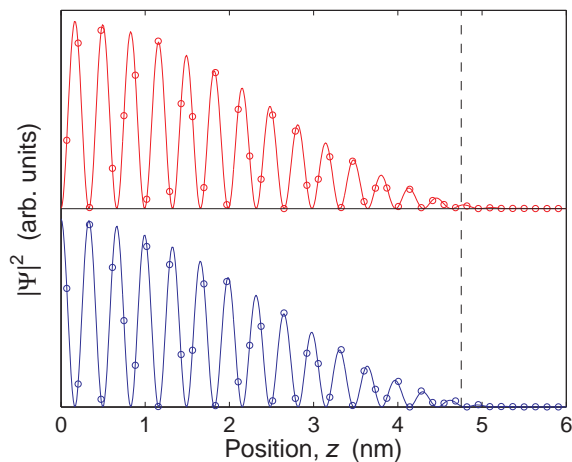


FIG. 1: (Color online.) Comparison of effective mass and tight binding results for the two lowest eigenstates in a  $\text{Si}_{0.7}\text{Ge}_{0.3}/\text{Si}/\text{Si}_{0.7}\text{Ge}_{0.3}$  quantum well of width 9.5 nm. (Only half the eigenfunctions are shown.) The solutions correspond to the same orbital subband, but different valley states. Bottom: ground state. Top: excited state. Solid lines: effective mass theory. Circles: tight-binding theory. Dashed line: quantum well boundary.

expressed as

$$\Psi(\mathbf{r}) = \sum_{j=\pm z} \alpha_j e^{ik_j z} u_{\mathbf{k}_j}(\mathbf{r}) F_j(\mathbf{r}). \quad (2)$$

The constants  $\alpha_j$  describe the relative phase between the two  $z$  valleys, with  $|\alpha_{+z}| = |\alpha_{-z}| = 1/\sqrt{2}$ . The functions  $e^{ik_j z} u_{\mathbf{k}_j}(\mathbf{r})$  are Bloch functions, where  $\mathbf{k}_{\pm z} = \pm k_0 \hat{z}$  are the conduction valley minima. We shall see that the envelope functions  $F_j(\mathbf{r})$  are the same for the two  $z$  valleys.

A central feature of the EM formalism, which is a consequence of Eq. (1), is that wavefunction separates neatly into atomic scale oscillations (the Bloch functions) and long wavelength modulations (the envelope function). This is apparent in Fig. 1, where we show the EM and TB results for the two valley states corresponding to the lowest subband of a quantum well, treating the Bloch functions as described in Sec. IV. The two wavefunctions have the same envelope, but their fast oscillations are phase shifted by  $\pi/2$ . Note that although the EM and TB approaches are fundamentally different (discrete vs. continuous), their wavefunction solutions are almost identical. Also note that the fast oscillations arising from  $u_{\mathbf{k}_j}(\mathbf{r})$  (not pictured in Fig. 1) are commensurate with the crystal lattice, while the oscillations from  $e^{ik_j z}$  are not, since  $k_0$  is not at the Brillouin zone boundary.

We can draw two main conclusions from the EM/TB comparison. First, the EM treatment correctly captures the essence of the subband physics, including both the long-wavelength and atomic scale features. Higher subbands (not pictured in Fig. 1) are also described accurately. Second, the main difference between pairs of valley states does not occur in the envelope function, but in

the fast oscillations. To leading order, the valley states are fully characterized by their valley composition vectors  $\boldsymbol{\alpha} = (\alpha_{-z}, \alpha_{+z})$ . Since the envelope function is independent of the valley physics at this order, the  $\boldsymbol{\alpha}$  vectors may be obtained from first-order, degenerate perturbation theory, by treating the valley coupling as a perturbation.<sup>36</sup> We now describe the perturbation theory, following the approach of Ref. [22], where shallow donors in silicon were considered. We specifically avoid the question of what causes valley splitting, since this lies outside the scope of the EM theory. Instead, we introduce valley coupling phenomenologically, through the parameter  $v_v$  described below.

In the EM formulation of Fritzsche and Tzose,<sup>37,38</sup> the strained silicon wavefunction, Eq. (2), is determined from the equation

$$0 = \sum_{j=\pm z} \alpha_j e^{-ik_j z} [H_0 + V_v(z) - \epsilon] F_j(z). \quad (3)$$

Here,

$$H_0 = T(z) + V_{\text{QW}}(z) + V_\phi(z), \quad (4)$$

and

$$T = -\frac{\hbar^2}{2} \frac{\partial}{\partial z} \left( \frac{1}{m_l} \frac{\partial}{\partial z} \right) \quad (5)$$

is the one-dimensional kinetic energy operator. The longitudinal effective mass  $m_l$  is materials dependent, and varies from layer to layer in the heterostructure. However, for Si-rich SiGe layers,  $m_l$  depends only weakly on the composition. We therefore take  $m_l \simeq 0.92 m_0$  to be a constant. Note that the transverse effective mass  $m_t$  does not appear in Eq. (5), since we initially consider only one-dimensional problems. In Sec. VIII, a more complicated, two-dimensional problem is studied, in which  $m_t$  appears.

Three different potential energies appear in Eqs. (3) and (4).  $V_{\text{QW}}(z)$  describes the conduction band offsets in the heterostructure. For a quantum well,  $V_{\text{QW}}(z)$  corresponds to a pair of step functions. The electrostatic potential energy  $V_\phi(z)$  describes any additional, slowly varying potential. Typically,  $V_\phi(z) \sim -eEz$  is an electrostatic potential caused by modulation doping in the heterostructure or by external gates.

The EM approximation breaks down near a singular confining potential like  $V_{\text{QW}}(z)$ , leading to a valley coupling. Very near the singularity, criterion (1) is not satisfied, and it becomes impossible to fully separate the short-wavelength physics of the crystal matrix from the long-wavelength confinement of the excess electron. However, we may neatly capture the valley interaction in terms of an effective coupling potential  $V_v(z)$ , which vanishes everywhere except within about an atomic length scale of the interface. The detailed form of such a coupling may be quite complicated.<sup>20</sup> However, because it is so strongly peaked, we may treat  $V_v(z)$  as a  $\delta$ -function

over EM length scales. Indeed, the  $\delta$ -function formulation arises naturally from some first principles theories of valley coupling at heterostructure interfaces.<sup>39</sup> We then have

$$V_v(z) = v_v \delta(z - z_i), \quad (6)$$

where  $z_i$  is the vertical position of the heterostructure interface. In Sec. VIII, we consider a case where  $z_i$  depends on the lateral position,  $x$ . However, in the other sections of the paper, we assume that  $z_i$  is constant. The valley interaction potential  $V_v(z)$  plays a role analogous to the central cell potential for an electron near a shallow donor.<sup>22</sup> The valley coupling strength  $v_v$  is a scalar quantity, which must be determined from experiments, or from atomistic methods like TB.

At lowest order in the perturbation theory (zeroth order), we set  $V_v(z) = 0$  in Eq. (3). Because of the fast oscillations associated with the exponential factors, the contributions from the two valleys are approximately decoupled at this level, reducing Eq. (3) the conventional Kohn-Luttinger envelope equation:

$$\left[ -\frac{\hbar^2}{2m_l} \frac{\partial^2}{\partial z^2} + V_{\text{QW}}(z) + V_\phi(z) \right] F^{(0)}(z) = \epsilon^{(0)} F^{(0)}(z). \quad (7)$$

Here, the superscript  $(0)$  denotes an unperturbed eigenstate. Note that the effective mass is the same for both  $z$  valleys. The corresponding envelopes are therefore equivalent, and we shall drop the valley index.

We now solve for  $\alpha$  and  $\epsilon$  in Eq. (3) using first order perturbation theory. By replacing  $F_j(z)$  in Eq. (3) with its zeroth order approximation, left-multiplying by  $F^{(0)*}(z) e^{ik_l z}$ , and integrating over  $z$ , we can express Eq. (3) in matrix form:

$$\begin{pmatrix} \epsilon^{(0)} + \Delta_0 & \Delta_1 \\ \Delta_1^* & \epsilon^{(0)} + \Delta_0 \end{pmatrix} \begin{pmatrix} \alpha_{-z} \\ \alpha_{+z} \end{pmatrix} = \epsilon \begin{pmatrix} \alpha_{-z} \\ \alpha_{+z} \end{pmatrix}. \quad (8)$$

We have dropped small terms involving atomic scale oscillations in the integrand. The perturbation terms are defined as follows:

$$\Delta_0 = \int V_v(z) |F^{(0)}(z)|^2 dz, \quad (9)$$

$$\Delta_1 = \int e^{-2ik_0 z} V_v(z) |F^{(0)}(z)|^2 dz. \quad (10)$$

Diagonalizing Eq. (8) gives the first order energy eigenvalues

$$\epsilon_{\pm} = \epsilon^{(0)} + \Delta_0 \pm |\Delta_1|, \quad (11)$$

and the valley splitting

$$E_v = 2|\Delta_1|. \quad (12)$$

In the valley basis  $(\alpha_{-z}, \alpha_{+z})$ , the eigenvectors corresponding to  $\epsilon_{\pm}$  are given by

$$\alpha_{\pm} = \frac{1}{\sqrt{2}} \begin{pmatrix} e^{i\theta/2} \\ \pm e^{-i\theta/2} \end{pmatrix}. \quad (13)$$

Here,  $\pm$  refers to the even or odd valley combinations, and we have defined the phases

$$e^{i\theta} \equiv \Delta_1 / |\Delta_1|. \quad (14)$$

For the case of a single interface at  $z = z_i$ , we obtain

$$\Delta_0 = v_v |F^{(0)}(z_i)|^2, \quad \Delta_1 = v_v e^{-2ik_0 z_i} |F^{(0)}(z_i)|^2. \quad (15)$$

We see that it is the magnitude of the envelope function at the interface that determines the strength of the valley coupling. The  $\alpha_{\pm}$  vectors for this geometry are obtained from Eq. (13), with

$$\theta = 2k_0 z_i. \quad (16)$$

The valley coupling integrals in Eqs. (9) and (10) provide a simple but economical characterization of the valley splitting. The coupling parameter  $v_v$ , which we compute below, provides a means to incorporate important microscopic details about the interface. The utility of the present theory is demonstrated by the ease with which we obtain results in the following sections. The accuracy of the theory is demonstrated in terms of the agreement between the EM and TB techniques.

We close this section by noting that several authors have criticized the Fritzsche-Twose formulation of the multi-valley EM theory,<sup>18,40</sup> particularly because of the way intervalley kinetic energy terms are calculated.<sup>26</sup> However, we emphasize that the present treatment includes all first order corrections to the valley splitting. Since the intervalley kinetic energy is of order  $v_v^2$ , it has a weaker contribution. The previous criticisms therefore do not apply here.

#### IV. TIGHT-BINDING THEORY

We now discuss a tight binding method for modeling heterostructures in silicon. Our main goal is to compare the solutions from such an atomistic technique with those of the EM theory, and to compute the valley coupling parameter  $v_v$ , whose value cannot be determined within the present EM theory. We focus on the two-band TB model of Boykin *et al.*,<sup>23,24</sup> because of its simplicity.

In the two-band model, the TB Hamiltonian includes nearest neighbor and next-nearest neighbor tunnel couplings,  $v$  and  $u$ , respectively. The values  $v = 0.683$  eV and  $u = 0.612$  eV are chosen such that (i) the bulk dispersion relation  $\epsilon(k)$  has two valleys, centered at  $|k| = k_0 = 0.82 (2\pi/a)$ , and (ii) the curvature of  $\epsilon(k)$  at the bottom of a valley gives the correct longitudinal effective mass  $m_l = 0.91 m_0$ . The unit cell in this theory consists of two atoms, with separation  $a/4$  along the [001] axis, where  $a = 5.431$  Å is the length of the silicon cubic unit cell. These parameters correspond to bulk silicon. A more sophisticated theory should take into account compositional variations and strain conditions. However, for most situations of interest, the modified parameters differ only slightly from the bulk.

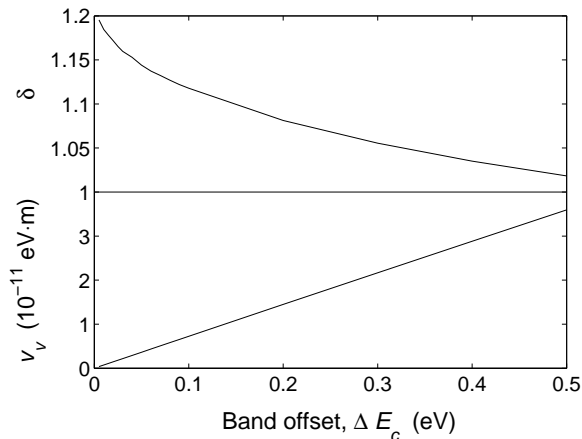


FIG. 2: The valley coupling parameter  $v_v$  and the quantum well “set-back” parameter  $\delta$ , defined in Eq. (27), as a function of the conduction band offset  $\Delta E_c$ . The results are obtained for a symmetric, finite square well by comparing the EM and TB theories.

In addition to the tunnel couplings  $v$  and  $u$ , we can also include onsite parameters  $\lambda_i$ , to provide a locally varying confinement potential. Both the conduction band offset  $V_{QW}(z)$  and the electrostatic potential  $V_\phi(z)$  can be expressed as on-site terms. To avoid boundary errors, we choose a TB lattice much larger than the confined electronic wavefunction. Diagonalization of the resulting TB Hamiltonian gives energy eigenvalues, from which we can calculate the valley splitting.

The two-band TB theory describes silicon valley physics with a minimal number (2) of input parameters, which are both fixed by fitting to measured band structure parameters. More sophisticated techniques can provide numerical improvements, but they generally do not capture any new physics. In Ref. [23], a comparison of the valley splitting between the two-band theory and a detailed many-band theory shows excellent qualitative agreement. The more accurate treatment gives results that are smaller by an approximately constant factor of 25%.

Some typical TB eigenstates for a finite square well are shown in Fig. 1. The data points correspond to the squared TB amplitudes plotted at the atomic sites. Comparison with the full EM wavefunctions requires knowledge of the Bloch functions in Eq. (2). However, to make contact with the TB results, we only need to evaluate the Bloch functions at the atomic sites. According to Eqs. (2) and (26) (see Sec. V, below), the low-lying valley pair of EM wavefunctions can be expressed as

$$\Psi_{\pm}(z) = \frac{1}{\sqrt{2}} [u_{-k_0}(\mathbf{r})e^{-ik_0z} \pm u_{+k_0}(\mathbf{r})e^{+ik_0z}] F(z), \quad (17)$$

where the ground-state alternates between  $+$  and  $-$  as a function of  $L$ . We can denote the two atoms in the TB unit cell as  $A$  and  $B$ , with the corresponding Bloch functions  $u_{k_0}(A)$  and  $u_{k_0}(B)$ . By translational symmetry, we

must have  $u_{k_0}(A) = \pm u_{k_0}(B)$ . (Typically, we observe the  $-$  sign in our TB analyses.) The Bloch functions satisfy time-reversal symmetry, so that  $u_{k_0}^*(\mathbf{r}) = u_{-k_0}(\mathbf{r})$ . Thus, defining  $u_{k_0}(A) = |u_{k_0}(A)|e^{i\varphi}$  and assuming proper normalization, we see that the squared TB amplitudes must fall on the curves

$$|\Psi_+(z)|^2 = 2 \cos^2(k_0z + \varphi)F^2(z) \quad (18)$$

$$|\Psi_-(z)|^2 = 2 \sin^2(k_0z + \varphi)F^2(z), \quad (19)$$

where all information about the Bloch functions is reduced to the unimportant phase variable  $\varphi$ . Eqs. (18) and (19) are plotted in Fig. 1, setting  $\varphi = 0$ . We see that these analytical forms provide an excellent representation of the TB results. However, we emphasize that Eqs. (18) and (19) are accurate only at the atomic sites. To describe the wavefunction between the atomic sites would require additional knowledge of the silicon Bloch functions.<sup>41,42,43,44</sup>

We can use the TB theory to determine the EM valley coupling parameter  $v_v$  by comparing corresponding results in the two theories. This is accomplished in Sec. V for the finite square well geometry, with results shown in Fig. 2.

## V. FINITE SQUARE WELL

We consider a symmetric square well with barrier interfaces at  $z_i = \pm L/2$ , corresponding to a quantum well of width  $L$ . We assume that the two interfaces are equivalent, so the same valley coupling  $v_v$  can be used on both sides. Using EM theory, the resulting valley splitting is

$$E_v = 4v_v F^2(L/2) |\cos(k_0L)|. \quad (20)$$

An analytical solution of the EM equations for the envelope function of a finite square well can be obtained by matching wavefunction solutions at the interfaces,<sup>32</sup> giving

$$F(L/2) = \left[ \frac{1}{k_b} + \frac{k_w L + \sin(k_w L)}{2k_w \cos^2(k_w L/2)} \right]^{-1/2}, \quad (21)$$

where

$$k_b = k_w \tan(k_w L/2). \quad (22)$$

The wavevector  $k_w$  can be obtained numerically from the transcendental equation

$$k_w^2 = \frac{2m_t \Delta E_c}{\hbar^2} \cos^2(k_w L/2). \quad (23)$$

Some typical results for the valley splitting as a function of the well width are shown in Fig. 3.

An approximate solution for Eqs. (20)-(23) can be obtained in the limit of a very deep or a very wide quantum

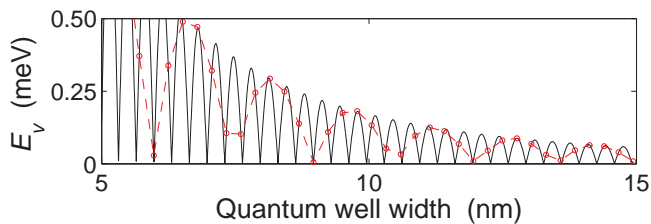


FIG. 3: (Color online.) Valley splitting in a finite square well. We compare effective mass results (solid curve) with tight binding results (circles), as a function of the quantum well widths  $L$  and  $L'$ , respectively (see text). The TB data points occur at integer multiples of the TB unit cell. We assume a  $\text{Si}_{0.7}\text{Ge}_{0.3}/\text{Si}/\text{Si}_{0.7}\text{Ge}_{0.3}$  quantum well, corresponding to  $\Delta E_c = 160$  meV.

well. When  $\pi^2 \hbar^2 / 2m_l L^2 \ll \Delta E_c$ , we find that  $k_w \simeq \pi/L$  for the first subband, leading to

$$F^2(L/2) \simeq \frac{\pi^2 \hbar^2}{m_l \Delta E_c L^3}. \quad (24)$$

The valley splitting is then given by

$$E_v \simeq \frac{4v_v \pi^2 \hbar^2}{m_l \Delta E_c L^3} |\cos(k_0 L)|. \quad (25)$$

This agrees with the dependence on well width obtained in Refs. [23] and [28], for an infinite square well.

Diagonalization of the perturbation Hamiltonian in Eq. (8) gives the ground ( $g$ ) and excited ( $x$ ) valley state  $\alpha$  vectors

$$\begin{aligned} \alpha_g &= (1, -\text{sign}[\cos(k_0 L)])/\sqrt{2} \quad (\text{ground}), \\ \alpha_x &= (1, \text{sign}[\cos(k_0 L)])/\sqrt{2} \quad (\text{excited}), \end{aligned} \quad (26)$$

where we have defined  $\text{sign}[x] \equiv x/|x|$ . These results are equivalent to Eq. (13), up to an overall phase factor. We see that the oscillations in Fig. 3 correspond to alternating even and odd ground states [ $\alpha_+ = (1, 1)/\sqrt{2}$  and  $\alpha_- = (1, -1)/\sqrt{2}$ , respectively], as a function of  $L$ . This alternating behavior has been observed previously in TB analyses.<sup>23</sup>

We can use these results to obtain an estimate for the valley coupling parameter  $v_v$ , by comparing the EM and TB results for the finite square well. For the EM case, we first solve Eq. (23) numerically, to obtain  $k_w$ . We then solve Eq. (21) for  $F(L/2)$ , finally obtaining the valley splitting from Eq. (20). For a given value of  $\Delta E_c$ , we fit Eq. (20) to the numerical TB results, as a function of  $L$ , using  $v_v$  as a fitting parameter. However, there is an ambiguity in relating the quantum well width,  $L$ , in the continuous EM theory to the discretized width,  $L' = Na/2$ , in the TB theory, where  $N$  is the number of silicon TB unit cells in the quantum well. For example, is the interface located on the last atomic site in the quantum well, the first atomic site in the barrier region, or somewhere in between? We see that the two widths,  $L$  and  $L'$ , may differ on the scale of a single atomic layer,

or  $a/4 = 1.36$  Å. To allow for this, we introduce a second fitting parameter  $\delta$ , as defined by

$$L = L' + \delta a/4. \quad (27)$$

With these two fitting parameters,  $v_v$  and  $\delta$ , we obtain nearly perfect correspondence between the EM and TB theories, as shown in Fig. 3.

In this manner, we can map out  $v_v$  and  $\delta$  as a function of  $\Delta E_c$ , giving the results shown in Fig. 2. We find that  $v_v(\Delta E_c)$  is linear over its entire range, with

$$v_v = 7.2 \times 10^{-11} \Delta E_c. \quad (28)$$

Here,  $v_v$  is given in units of eV·m when  $\Delta E_c$  is expressed in units of eV. As described in Sec. IV, a many-band TB analysis obtains results for  $v_v$  that are smaller by a factor of about 25%.

From Fig. 2, we see that  $\delta \simeq 1.1$  forms a reasonable approximation over the typical experimental range,  $\Delta E_c \simeq 50$ -200 meV. This corresponds to about one atomic layer, or half an atomic layer on either side of the quantum well. We can interpret  $\delta$  as the set-back distance for an effective scattering barrier which causes valley coupling. A similar interpretation was given for the parameter  $\alpha$  in Ref. [29]. We see that this set-back distance increases for a shallow quantum well.

Finally, we consider the asymptotic limits of our EM theory. In the limit  $\Delta E_c \rightarrow \infty$ , corresponding to an infinite square well, Eq. (25) becomes exact. Since  $E_v$  does not vanish, we conclude that  $v_v \propto \Delta E_c$  in this limit. This is precisely the behavior observed in Fig. 2.

In the limit  $\Delta E_c \rightarrow 0$ , corresponding to a shallow square well, Eq. (25) is not valid. Instead, we obtain  $F^2(L/2) \simeq \Delta E_c L m_l / \hbar^2$ , leading to  $E_v \simeq 2\Delta E_c L v_v m_l \cos(k_0 L) / \hbar^2$ . In this limit, we expect the valley splitting to vanish, but we can make no other predictions about  $v_v$ . The numerical results, however, suggest that the linear dependence of  $v_v(\Delta E_c)$  extends smoothly to zero.

## VI. QUANTUM WELL IN AN ELECTRIC FIELD

We now consider a quantum well in the presence of an electric field oriented in the growth direction. The geometry is shown in the inset of Fig. 4. For physically realistic fields, caused by modulation doping or electrical top-gates, the resulting electrostatic potential satisfies the EM criterion, Eq. (1). We therefore proceed as in Sec. V, using the numerical values for  $v_v(\Delta E_c)$ , obtained for a symmetric square well. The electrostatic potential enters our analysis through the envelope equation (8). Although there are no exact solutions for the problem of a tilted square well, the approximate treatment described here provides analytic results that accurately reproduce the results of TB theory.

We assume an electrostatic potential energy given by  $V_\phi(z) = -eEz$ , and a quantum well of width  $L$  and height

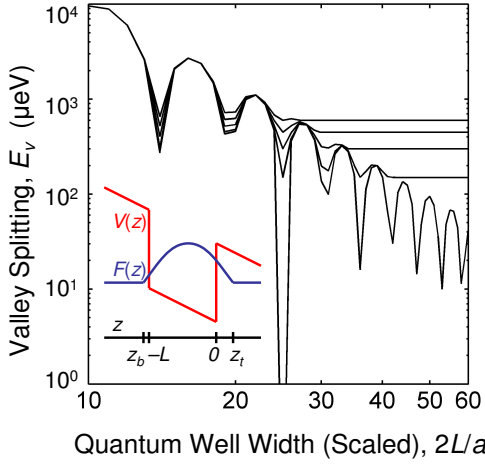


FIG. 4: (Color online.) Effective mass results for the valley splitting in an electric field, as a function of the quantum well width. Five  $E$  fields are shown, from bottom to top:  $E = 0, 1.04, 2.08, 3.12,$  and  $4.16$  MV/m. The well width  $L$  is scaled by the TB unit cell size,  $a/2 = 2.716$  Å. Results are shown for a  $\text{Si}_{0.8}\text{Ge}_{0.2}/\text{Si}/\text{Si}_{0.8}\text{Ge}_{0.2}$  quantum well, analogous to Fig. 1(a) of Ref. [23]. Inset:  $E$ -field geometry, with confinement potential  $V(z) = V_{\text{QW}}(z) + V_{\phi}(z)$  and variational wavefunction  $F(z)$  given in Eq. (29). Here,  $z_b = z_t - \pi/k$ .

$\Delta E_c$ . The top barrier of the well lies at  $z = 0$ . We consider the following variational envelope function:

$$F(z) = \begin{cases} -\sqrt{\frac{2k}{\pi}} \sin[k(z - z_t)] & (z_t - \frac{\pi}{k} < z < z_t) \\ 0 & (\text{otherwise}). \end{cases} \quad (29)$$

For simplicity, we have chosen a wavefunction tail that terminates abruptly. This approximation is satisfactory for a variational calculation, since the tail, which is exponentially suppressed, contributes very little to the energy expectation value.

In our trial function, the parameter  $k$  accounts for the finite barrier height by allowing the wavefunction to extend into the barrier region. The upward shift of the wavefunction in the presence of an electric field is given by  $z_t$ . The solution (29) becomes exact for an infinite square well at zero field, suggesting that the trial function will be most effective in this limit. We therefore define the small parameters

$$x = \frac{\hbar^2 \pi^2}{2m_l L^2 \Delta E_c} \quad \text{and} \quad y = \frac{eEL}{4\Delta E_c}. \quad (30)$$

The energy expectation value, obtained from envelope equation (2), can be expressed in terms of the dimensionless variational parameters

$$\theta_1 = kL \quad \text{and} \quad \theta_2 = kz_t, \quad (31)$$

giving

$$\frac{\pi^2 \epsilon}{\Delta E_c} \simeq \begin{cases} x\theta_1^2 - 4\pi^2 y(\theta_2 - \pi/2)/\theta_1 + 2\pi[\theta_2^3 - (\theta_1 + \theta_2 - \pi)^3]/3 & (\theta_1 + \theta_2 < \pi) \\ x\theta_1^2 - 4\pi^2 y(\theta_2 - \pi/2)/\theta_1 + 2\pi\theta_2^3/3 & (\theta_1 + \theta_2 \geq \pi). \end{cases} \quad (32)$$

In the first case in Eq. (32), the wavefunction extends past both barriers. For large enough electric fields ( $y > x$ ), the wavefunction only extends past one barrier (see inset of Fig. 4). Minimization of  $\epsilon$  with respect to  $\theta_1$  and  $\theta_2$  gives

$$\left. \begin{aligned} \theta_1 &\simeq \pi + \sqrt{x-y} - \sqrt{x+y} \\ \theta_2 &\simeq \sqrt{x+y} \end{aligned} \right\} \quad (x > y), \quad (33)$$

$$\left. \begin{aligned} \theta_1 &\simeq \pi(y/x)^{1/3} \\ \theta_2 &\simeq (8y^2x)^{1/6} \end{aligned} \right\} \quad (x \leq y), \quad (34)$$

where we have made use of the fact that  $\theta_2 \ll \pi$ . For the case  $x > y$ , we have also used  $\pi - \theta_1 \ll \pi$ .

To compute the valley splitting, we use the results  $F^2(-L) \simeq 2(\pi - \theta_1 - \theta_2)^2/L$  and  $F^2(0) \simeq 2\theta_2^2/L$  when

$x > y$ , and  $F^2(0) \simeq 2\theta_2^2\theta_1/\pi L$  when  $x \leq y$  to obtain

$$E_v L \simeq \begin{cases} 4v_v |e^{ik_0 L}(x-y) + e^{-ik_0 L}(x+y)| & (x > y) \\ 8v_v y & (x \leq y). \end{cases} \quad (35)$$

These solutions are plotted in Fig. 4 as a function of the quantum well width for several different  $E$  fields. In the figure, we have evaluated Eq. (35) only at integer multiples of the TB unit cell, to facilitate comparison with Fig. 1(a) in Ref. [23]. The correspondence between the EM and TB theories is quantitatively and qualitatively accurate, particularly for large well widths.

In Fig. 4, we see that the crossover to high field behavior corresponds to  $E_v$  becoming independent of  $L$ . The crossover occurs when  $y > x$  or

$$E > \frac{2\pi^2 \hbar^2}{m_l e L^3}. \quad (36)$$



At low fields, the valley splitting exhibits interference oscillations, similar to Fig. 3. At high fields, the envelope function no longer penetrates the barrier on the bottom side of the quantum well. The top and bottom barriers then no longer produce interfering contributions to the valley splitting, causing the oscillations in  $E_v(L)$  to cease. Since we have chosen a trial wavefunction with no tail, the crossover to high field behavior in Fig. 4 occurs abruptly. This is in contrast with the TB results where small oscillations can still be observed right above the crossover.

We now study the asymptotic behaviors of Eq. (35). In the zero field limit,  $y \rightarrow 0$ , Eq. (35) correctly reduces to Eq. (25) for a symmetric square well. In the high field limit, we can ignore the bottom barrier entirely. For an infinite barrier, the problem is often analyzed using the Fang-Howard trial wavefunction.<sup>32</sup> To make contact with this approach, we shall now perform a modified Fang-Howard analysis, and demonstrate a correspondence between the two results.

The conventional Fang-Howard trial function does not penetrate the barrier region. However, for a finite barrier height  $\Delta E_c$ , it is the amplitude of the wavefunction at the interface which determines the valley splitting. We must therefore modify the Fang-Howard trial function to allow the wavefunction to penetrate the top barrier, similar to Eq. (29). An appropriately modified trial function is given by

$$F(z) = \begin{cases} -\sqrt{b^3/2}(z - z_t) \exp[b(z - z_t)/2] & \text{for } z < z_t \\ 0 & \text{for } z \geq z_t \end{cases}. \quad (37)$$

This is just the usual Fang-Howard variational function, shifted upward by  $z_t$ . In the Fang-Howard approach, the wavefunction tail decays exponentially into the lower portion of the quantum well. This treatment is more physical than the abrupt termination assumed in Eq. (29). However, the tail contribution to the variational calculation is insignificant, to leading order. Following the conventional Fang-Howard approach, but now using  $b$  and  $z_t$  as variational parameters, we obtain

$$E_v = \frac{2v_v eE}{\Delta E_c}. \quad (38)$$

As in the case of a symmetric square well, we see that  $E_v \propto \Delta E_c^{-1}$ . We also find that Eq. (38) is equivalent to the high-field limit of Eq. (35). Thus, the non-oscillating, high-field portions of the curves in Fig. 4 correspond to the ‘‘Fang-Howard limit’’ described by Eqs. (37) and (38). This agreement demonstrates that the variational form of Eq. (29) is robust over the entire field range.

## VII. VALLEY SPLITTING IN A 2DEG

In this section and the next, we consider problems of particular experimental importance. In both cases, conventional techniques like TB theory are somewhat cum-

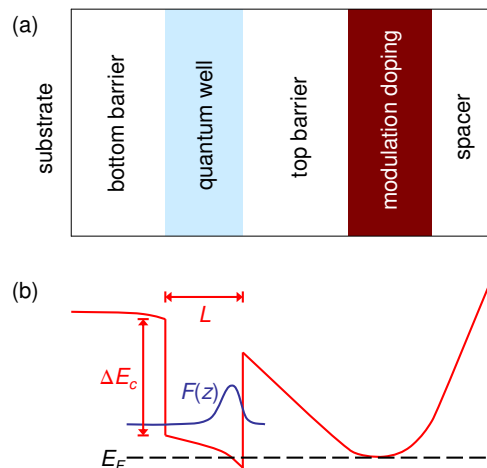


FIG. 5: (Color online.) Typical 2DEG structure for a SiGe/Si/SiGe quantum well. (a) Heterostructure, left to right: strain-relaxed SiGe substrate and barrier, strained silicon quantum well, strain-relaxed SiGe barrier,  $n^+$  SiGe doping layer, and SiGe spacer layer. (b) Conduction band profile, showing the envelope function  $F(z)$  and the Fermi energy  $E_F$ .

bersome. However, the EM formalism leads to straightforward solutions. We first consider a two-dimensional electron gas (2DEG) in a SiGe/Si/SiGe quantum well, which extends the single electron scenarios we have studied so far, by including many-body interactions.

We consider the modulation-doped heterostructure shown in Fig. 5(a). In this structure, we assume that the charge is found only in the 2DEG and the doping layers. A more detailed analysis could also include background charge and charge trapped at an interface. Because the modulation doping field is large in a typical heterostructure, we will ignore the bottom barrier in our calculations. The conduction band profile is sketched in Fig. 5(b). We treat many-body interactions using the Hartree approximation, as common for a quantum well. However, other many-body interactions can also be included,<sup>18,45</sup> using similar techniques to calculate the valley splitting.

The modified Fang-Howard approach gives a reasonable approximation for an electron in a 2DEG.<sup>18</sup> However, we must include the electron-electron interactions self-consistently. Within the Hartree approximation,<sup>32</sup> the 2DEG charge density  $\rho(z)$  is given by

$$\rho(z) = -enF^2(z), \quad (39)$$

where  $n$  is the density of the 2DEG and  $F(z)$  is defined in Eq. (37). The charge density is related to the electrostatic potential through the Poisson equation,

$$\frac{d^2 \phi_H}{dz^2} = -\frac{\rho}{\epsilon}, \quad (40)$$

where  $\epsilon$  is the dielectric constant of silicon. The bound-



ary conditions on Eq. (40) are given by

$$\begin{aligned} d\phi_H/dz &= 0 & (z \rightarrow -\infty), \\ \phi_H &= 0 & (z = 0). \end{aligned} \quad (41)$$

The second boundary condition anchors the energy of the confinement potential,  $V_{\text{QW}}(z)$ , at top of the quantum well.<sup>32</sup> The corresponding electrostatic potential is given by

$$\begin{aligned} \phi_H(z) = \frac{en}{2b\epsilon} \left\{ [b^2(z - z_t)^2 - 4b(z - z_t) + 6]e^{b(z-z_t)} \right. \\ \left. - [b^2z_t^2 + 4bz_t + 6]e^{-bz_t} \right\} \end{aligned} \quad (42)$$

The variational parameters are determined by minimizing the total energy per electron, given by

$$\epsilon = \langle T \rangle + \frac{1}{2}\langle V_\phi \rangle + \langle V_{\text{QW}} \rangle. \quad (43)$$

Here,  $V_\phi(z)$  corresponds to the Hartree potential  $-e\phi_H(z)$ . The factor of 1/2 in the Hartree term prevents overcounting of the interactions.<sup>32</sup> Note that, in contrast with calculations for Si/SiO<sub>2</sub> inversion layers, we do not include any contributions from image potentials in Eq. (43), since the dielectric constants for Si and SiGe are nearly equal, and any other interfaces that could produce images are far away from the 2DEG.

We evaluate Eq. (43), obtaining

$$\epsilon \simeq \frac{\hbar^2 b^2}{8m_l} + \frac{e^2 n}{4b\epsilon} \left( \frac{33}{8} - 2bz_t \right) + \frac{\Delta E_c b^3 z_t^3}{6}, \quad (44)$$

where we have made use of the dimensionless small parameters  $bz_t$  and  $e^2 n / \epsilon \Delta E_c b$ . The first of these describes the shift of the wavefunction towards  $+\hat{z}$ , while the second describes the relative magnitude of the electrostatic energy with respect to the band offset  $\Delta E_c$ . Minimization of  $\epsilon$  with respect to  $b$  and  $z_t$  gives

$$z_t^2 \simeq \frac{8\hbar^2}{33m_l \Delta E_c} \quad \text{and} \quad b^3 \simeq \frac{33e^2 n m_l}{8\hbar^2}. \quad (45)$$

We can now calculate the valley splitting for a 2DEG. Under the previous approximations, we obtain a very simple expression for the wavefunction at the top quantum well interface,

$$F^2(0) \simeq \frac{e^2}{2\epsilon \Delta E_c}, \quad (46)$$

leading to the valley splitting

$$E_v = \frac{v_v e^2 n}{\epsilon \Delta E_c}. \quad (47)$$

[Note that this result is obtained for a perfectly smooth interface. As we show in Sec. VIII, substrate roughness can reduce this estimate considerably. However, the scaling dependence in Eq. (47) remains valid.]

We can use our estimate for the valley coupling parameter, Eq. (28), to obtain a quantitative prediction for the

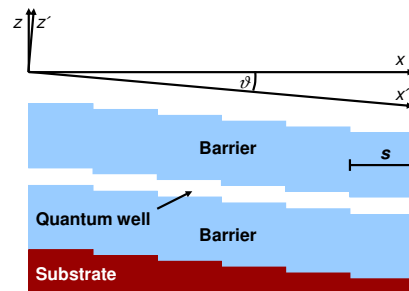


FIG. 6: (Color online.) Tilted quantum well geometry, with crystallographic axes  $(x, y, z)$  and rotated axes  $(x', y', z')$ , assuming  $y = y'$ . The effective tilt angle is  $\vartheta$ , and the atomic step size is  $s$ .

valley splitting in a 2DEG. Expressing the valley splitting in units of meV and the 2DEG density  $n$  in units of  $10^{12} \text{ cm}^{-2}$ , we find that

$$E_v \simeq 1.14 n. \quad (48)$$

Here, we have used the low-temperature dielectric constant for silicon,  $\epsilon = 11.4\epsilon_0$ . It is interesting to note that the barrier height  $\Delta E_c$  does not directly enter the final result.

We can compare Eq. (48) with the corresponding, non-self-consistent calculation, by treating the system of 2DEG and doping layer as a parallel plate capacitor with electric field  $E = en/\epsilon$ . The valley splitting for an electron in such a field is given in Eq. (38), with the result

$$E_v \simeq 2.29 n \quad (\text{non-self-consistent}). \quad (49)$$

The factor of 2 difference with Eq. (48) arises because the electric field in a real 2DEG is not uniform, due to the presence of charge. The non-self-consistent procedure therefore uses an electric field that is too large, overall, and it overestimates the valley splitting.

In Eq. (48), the prefactor 1.14 can be compared with similar estimates for silicon inversion layers. Ohkawa and Uemura obtain a prefactor of 0.15,<sup>26,27</sup> while Sham and Nakayama obtain 0.33.<sup>46</sup> A recent experiment in a top-gated SiO<sub>2</sub>/Si/SiO<sub>2</sub> heterostructure has obtained a much larger value of the valley splitting.<sup>47</sup> However, several remarks are in order. First, we do not specifically consider top-gated structures here, so Eq. (48) does not directly apply to the latter experiment. Second, we point out that depletion and image charges, which were not considered here, play a more significant role in an inversion layer than a quantum well geometry. Finally, we note that a more accurate, many-band estimate for  $v_v$  would reduce the prefactor in Eq. (48) by about 25%, as discussed in Sec. IV.

### VIII. TILTED QUANTUM WELL IN A MAGNETIC FIELD

In high-mobility Si/SiGe devices, substrates are often intentionally tilted away from [001] by up to several degrees, to promote uniform epitaxial growth under strain conditions, and to help reduce step bunching. Additional roughening occurs during the growth of strained heterostructures. (Recent advances in nanomembrane technology may help overcome this difficulty.<sup>48</sup>) Typical devices therefore contain atomic steps at their surfaces and interfaces, associated with global or local tilting. At the EM level, one might expect to ignore such small, atomic-scale steps, and to work in the locally tilted basis  $(x', y', z')$  shown in Fig. 6. However, when valley coupling is taken into account, the problem becomes two-dimensional, since the tilted surface is misaligned with respect to the crystallographic axes. In such high dimensional geometries, there is an obvious scaling difficulty for atomistic theories. However, the EM theory of valley splitting has a definite, practical advantage. The following discussion expands upon our previous analysis in Ref. [49].

We consider a tilted quantum well in a magnetic field. In the low-field limit, the electronic wavefunction covers many steps, leading to interference effects in Eq. (10), and a near-total suppression of the valley splitting. To see this, we note that the vertical position of the interface,  $z_i$ , becomes a function of the lateral position,  $x$ . The phase factor in Eq. (10) is therefore not a constant, in contrast with the case of a flat interface. In Fig. 6, we assume that a single step corresponds to a change of one atomic plane, or  $a/4 = 1.36 \text{ \AA}$ . From Eq. (10), the phase shift between neighboring steps is given by  $2k_0(a/4) = 0.82\pi$ . So the steps are nearly  $180^\circ$  out of phase, and the interference is severe.

At low magnetic fields, the experimental data are consistent with this picture of suppressed valley splitting.<sup>6</sup> (The experiments also suggest a non-vanishing zero-field extrapolation, which we shall investigate elsewhere.<sup>50</sup>) Some of the characteristic features of the magnetic field dependence can be explained in terms of the lateral confinement of the electronic wavefunction. Magnetic confinement over the length scale  $l_B = \sqrt{\hbar}/|eB|$  reduces the number of steps that contribute to the valley splitting integral. The interference effects and the suppression of the valley splitting are similarly reduced. To get a sense of the scales involved, we note that a wavefunction of width  $4l_B$  will cover  $16(l_B/a) \tan \vartheta$  steps, where  $\vartheta$  is the local tilt angle in Fig. 6. (Here, we have assumed a wavefunction of diameter  $2\sqrt{\langle r^2 \rangle} = 4l_B$ , obtained using the solutions described below.) For a typical  $\vartheta = 2^\circ$  miscut,<sup>6</sup> the wavefunction covers about 26 steps when  $B = 1 \text{ T}$ , and 13 steps when  $B = 4 \text{ T}$ . The confinement provided by electrostatic top-gates can also enhance the valley splitting by reducing the step coverage.<sup>6</sup>

We can gain insight into the magnetic field dependence of the valley splitting by considering a simple model. We

first express the envelope function equation in the tilted basis  $(x', y', z')$ , giving

$$\left[ \sum_{n=1}^3 \frac{1}{2m_n} \left( -i\hbar \frac{\partial}{\partial x'_n} + eA_n(\mathbf{r}') \right)^2 + V_{\text{QW}}(z') \right] F(\mathbf{r}') = \epsilon F(\mathbf{r}'), \quad (50)$$

where  $m_1 = m_2 = m_t = 0.19m_0$  and  $m_3 = m_l = 0.92m_0$ , are the transverse and lateral effective masses, respectively. We note that the anisotropic effective masses are defined with respect to the crystallographic axes  $(x, y, z)$ , not the growth axes. The full effective mass tensor in Eq. (50) should therefore include off-diagonal terms. In particular, we should have a term proportional to  $m_{xz}^{-1} \simeq \vartheta(m_t^{-1} - m_l^{-1})$ , where we have taken  $\vartheta \ll \pi/2$ . For a  $2^\circ$  miscut, however, we find that  $m_t/m_{xz} = 0.028$ , so the off-diagonal term is much smaller than the diagonal terms. If desired, the off-diagonal corrections could be included, perturbatively. Here, we have considered only the leading order (diagonal) mass terms.

In Eq. (50), the magnetic field is introduced through the vector potential. We consider the symmetric gauge, with  $\mathbf{A}(\mathbf{r}') = (-y', x', 0)B/2$ . We also assume an approximate form for the quantum well potential  $V_{\text{QW}}(z')$ , which is smoothly tilted (*i.e.*, not step-like). This will be adequate for our simple estimate. Separation of variables then leads to solutions of form  $F(\mathbf{r}') = F_{xy}(x', y')F_z(z')$ , where  $F_z(z')$  is the quantum well wavefunction, studied elsewhere in this paper, and  $F_{xy}(x', y')$  is the lateral wavefunction given by<sup>32</sup>

$$F_{xy}^{(nl)}(r', \theta') = \sqrt{\frac{n!}{\pi l_B^2 2^{|l|+1} (n+|l|)!}} e^{il\theta'} \times e^{-r'^2/4l_B^2} \left( \frac{r'}{l_B} \right)^{|l|} L_n^{(|l|)} \left( \frac{r'^2}{2l_B^2} \right). \quad (51)$$

Here, we use radial coordinates, defined as  $(x', y') = (r' \cos \theta', r' \sin \theta')$ , while  $n = 0, 1, 2, \dots$  are the radial quantum numbers (the Landau level indices),  $l = 0, \pm 1, \pm 2, \dots$  are the azimuthal quantum numbers, and  $L_n^{(|l|)}(x)$  are associated Laguerre polynomials.<sup>51</sup> The energy eigenvalues for  $F_{xy}^{(nl)}(r', \theta')$  are given by

$$\epsilon_{nl} = \frac{2n + l + |l| + 1}{2} \hbar\omega_c, \quad (52)$$

where  $\omega_c = e|B|/m_t$  is the cyclotron frequency. Note that we have ignored spin physics here.

To take an example, we now focus on the lowest Landau level, with  $n = l = 0$ . The behavior of the valley splitting in higher Landau levels is considered elsewhere.<sup>31,52</sup> Eq. (51) now becomes

$$F_{xy}(x', y') = \frac{1}{\sqrt{2\pi l_B^2}} e^{-(x'^2 + y'^2)/4l_B^2}. \quad (53)$$

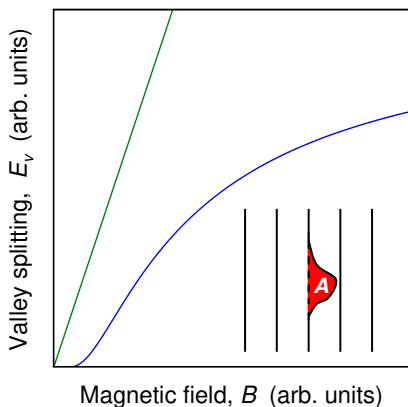


FIG. 7: (Color online.) Valley splitting on a tilted quantum well, in a magnetic field. The lower (blue) curve shows the exponential suppression of the valley splitting, Eq. (55), arising from perfectly uniform steps. The upper (green) curve shows the linear behavior arising from the “plateau” model of disordered steps. Inset shows a localized step fluctuation (or “wiggle”) of area  $A$ , as analyzed in the text.

We assume a strong electric field, so that only one quantum well interface contributes to the valley splitting. For a smoothly tilted interface, the valley interaction potential is given by

$$V_v(z') = v_v \delta(z'). \quad (54)$$

The valley splitting is then given by

$$\begin{aligned} E_v &\simeq \frac{v_v}{\pi l_B^2} \left| \int |F_z(z')|^2 e^{-r'^2/2l_B^2} e^{2ik_0 x' \vartheta} \delta(z') dx' dy' dz' \right| \\ &= 2v_v F_z^2(0) e^{-2(k_0 l_B \theta)^2}, \end{aligned} \quad (55)$$

where we have used the fact that  $z = -x' \sin \vartheta + z' \cos \vartheta \simeq -x' \vartheta$ , along the  $z' = 0$  interface.

The preceding results are obtained for perfectly uniform steps at a quantum well interface, which we approximate by a smooth, uniform tilt. The resulting magnetic field dependence of the valley splitting, first reported in Ref. [49], is shown in Fig. 7. The interference effect, arising from the interfacial tilt, drives the valley splitting to zero at small fields, as consistent with experimental observations. However, the exponential suppression of  $E_v$  in Eq. (55) is an anomalous feature caused by the absence of disorder. If we consider more realistic step geometries, including disorder in the step widths and profiles,<sup>53</sup> the valley splitting will be enhanced by orders of magnitude, as confirmed by simulations.<sup>49,54</sup>

We can obtain an estimate for the valley splitting enhancement due to fluctuations by considering a single step wiggle, as shown in the inset of Fig. 7. The correction to Eq. (55) is computed by noting that the area of the left step increases by  $A$ , while the right step decreases by  $A$ . We have shown that the phase difference between neighboring steps in the valley splitting integral is  $k_0 a/2$ .

The perturbed valley splitting integral is therefore given by

$$E_v \simeq |E_{v0} + 4e^{i\phi} A v_v F_z^2(0) F_{xy}^2(\mathbf{r}'_0) \sin(k_0 a/4)|. \quad (56)$$

Here, we have expressed the unperturbed result of Eq. (55) as  $E_{v0}$ , and we have assumed the amplitude of the envelope function is approximately constant across the wiggle at position  $\mathbf{r}' = \mathbf{r}'_0$ . We also note that the two terms in Eq. (56) enter the valley splitting integral with a phase difference  $\phi$  that depends on  $\mathbf{r}'_0$ . Let us approximate  $F_{xy}(\mathbf{r}'_0) \simeq 1/2\pi l_B^2$  and  $\sin(k_0 a/4) \simeq 1$ . Then the fluctuation contribution is

$$v_v F_z^2(0) \frac{2A}{\pi l_B^2}, \quad (57)$$

which has a linear dependence on the magnetic field. Therefore, at low fields, the fluctuation contribution dominates over the estimate obtained for a uniform tilt, Eq. (55). More realistic fluctuation models would include a distribution of fluctuations, with contributions that partially cancel out due to interference effects. However, the assumption of one dominant fluctuation loop (the “plateau” model<sup>49</sup>), leads to the linear dependence shown in Fig. 7, which is consistent with experiments. (To obtain correspondence with Ref. [49], we note that the “excess area” in that paper corresponds to  $2A$  in our notation.)

## IX. CONCLUSIONS

In this paper, we have developed an effective mass theory for the valley splitting of a strained SiGe/Si/SiGe quantum well. To compute the valley splitting of a perfect quantum well with no steps, one needs two input parameters that describe the location and curvature of the band minimum as well as the valley coupling constant  $v_v$  that captures the relevant microscopic details of the interfaces. These parameters must be obtained from a more microscopic theory, or from experiments. It is worth noting that, unlike bulk properties, the interface can vary from system to system, so that  $v_v$  should be determined for each case. In this work, we have used a simple tight binding theory to compute  $v_v$ , as a function of the conduction band offset  $\Delta E_c$ , assuming a sharp heterostructure interface. The results provide excellent agreement between the effective mass and tight binding theories.

Once  $v_v$  is known, we may apply the effective mass theory to a range of important problems. Here, we have considered the finite square well, with and without an applied electric field. We have also performed a self-consistent analysis of a 2DEG, using the Hartree approximation. Excellent agreement between effective mass and atomistic theories confirms our main conclusion, that the valley splitting in this system can be fully explained through a single coupling constant,  $v_v$ .

The effective mass theory is particularly useful for two or three-dimensional geometries, which cannot be easily treated in atomistic theories, due to scaling constraints. Here, we have applied the effective mass formalism to the inherently 2D problem of valley splitting in a magnetic field for a quantum well grown on a miscut substrate. We find that interference effects strongly suppress the valley splitting at low magnetic fields. However this suppression is reduced by introducing a small amount of disorder into the step-like geometry of the quantum well interface, as consistent with experimental evidence and simulations.

N.B. In the final stages of preparation of this manuscript, we became aware of Ref. [55], which presents

some similar results to those reported here.

### Acknowledgments

We would like to acknowledge stimulating discussions with M. A. Eriksson, G. Klimeck, A. Punnoose, and P. von Allmen. This work was supported by NSA under ARO contract number W911NF-04-1-0389 and by the National Science Foundation through the ITR (DMR-0325634) and EMT (CCF-0523675) programs.

- 
- \* Electronic address: Electronic mail: friesen@cae.wisc.edu
- <sup>1</sup> P. Weitz, R. J. Haug, K. von Klitzing, and F. Schäffler, *Surf. Sci.* **361/362**, 542 (1996).
  - <sup>2</sup> S. J. Koester, K. Ismail, and J. O. Chu, *Semicond. Sci. Technol.* **12**, 384 (1997).
  - <sup>3</sup> V. S. Khrapai, A. A. Shashkin, and V. P. Dolgoplov, *Phys. Rev. B* **67**, 113305 (2003).
  - <sup>4</sup> K. Lai, W. Pan, D. C. Tsui, S. Lyon, M. Mühlberger, and F. Schäffler, *Phys. Rev. Lett.* **93**, 156805 (2004).
  - <sup>5</sup> V. M. Pudalov, A. Punnoose, G. Brunthaler, A. Prinz, and G. Bauer, *cond-mat/0104347* (unpublished).
  - <sup>6</sup> S. Goswami, K. A. Slinker, M. Friesen, L. M. McGuire, J. L. Truitt, C. Tahan, L. J. Klein, J. O. Chu, P. M. Mooney, D. W. van der Weide, R. Joynt, S. N. Coppersmith, and M. A. Eriksson, to appear in *Nature Physics*, *cond-mat/0611221*.
  - <sup>7</sup> M. A. Eriksson, M. Friesen, S. N. Coppersmith, R. Joynt, L. J. Klein, K. Slinker, C. Tahan, P. M. Mooney, J. O. Chu, and S. J. Koester, *Quant. Inform. Process.* **3**, 133 (2004).
  - <sup>8</sup> L. P. Rokhinson, L. J. Guo, S. Y. Chou, and D. C. Tsui, *Microelectr. Engineer.* **63**, 147 (2002).
  - <sup>9</sup> M. Xiao, I. Martin, E. Yablonovitch, and H. W. Jiang, *Nature (London)* **430**, 435 (2004).
  - <sup>10</sup> I. Zutic, J. Fabian, and S. Das Sarma, *Rev. Mod. Phys.* **76**, 323 (2004)
  - <sup>11</sup> F. R. Bradbury, A. M. Tyryshkin, Guillaume Sabouret, Jeff Bokor, Thomas Schenkel, and S. A. Lyon, *Phys. Rev. Lett.* **97**, 176404 (2006).
  - <sup>12</sup> H. Sellier, G. P. Lansbergen, J. Caro, N. Collaert, I. Ferain, M. Jurczak, S. Biesemans, and S. Rogge, to appear in *Phys. Rev. Lett.*, *cond-mat/0608159*.
  - <sup>13</sup> B. E. Kane, *Nature (London)* **393**, 133 (1998).
  - <sup>14</sup> R. Vrijen, E. Yablonovitch, K. Wang, H. W. Jiang, A. Balandin, V. Roychowdhury, T. Mor, and D. DiVincenzo, *Phys. Rev. A* **62**, 012306 (2000).
  - <sup>15</sup> J. L. O'Brien, S. R. Schofield, M. Y. Simmons, R. G. Clark, A. S. Dzurak, N. J. Curson, B. E. Kane, N. S. McAlpine, M. E. Hawley, and G. W. Brown, *Phys. Rev. B* **64**, 161401 (2001).
  - <sup>16</sup> M. Friesen, P. Rugheimer, D. E. Savage, M. G. Lagally, D. W. van der Weide, R. Joynt, and M. A. Eriksson, *Phys. Rev. B* **67**, 121301 (2003).
  - <sup>17</sup> W. Kohn, in *Solid State Physics*, edited by F. Seitz and D. Turnbull (Academic Press, New York, 1957), Vol. 5.
  - <sup>18</sup> T. Ando, A. B. Fowler, and F. Stern, *Rev. Mod. Phys.* **54**, 437 (1982).
  - <sup>19</sup> P. Y. Yu and M. Cardona, in *Fundamentals of Semiconductors*, Third Edition (Springer-Verlag, Berlin, 2001).
  - <sup>20</sup> S. T. Pantelides and C. T. Sah, *Phys. Rev. B* **10**, 621 (1974).
  - <sup>21</sup> S. T. Pantelides, *Rev. Mod. Phys.* **50**, 797 (1978).
  - <sup>22</sup> M. Friesen, *Phys. Rev. Lett.* **94**, 186403 (2005).
  - <sup>23</sup> T. B. Boykin, G. Klimeck, M. A. Eriksson, M. Friesen, S. N. Coppersmith, P. von Allmen, F. Oyafuso, and S. Lee, *Appl. Phys. Lett.* **84**, 115 (2004).
  - <sup>24</sup> T. B. Boykin, G. Klimeck, M. Friesen, S. N. Coppersmith, P. von Allmen, F. Oyafuso, and S. Lee, *Phys. Rev. B* **70**, 165325 (2004).
  - <sup>25</sup> T. B. Boykin, G. Klimeck, P. von Allmen, S. Lee, and F. Oyafuso, *Journ. of Appl. Phys.* **97**, 113702 (2005).
  - <sup>26</sup> F. J. Ohkawa and Y. Uemura, *J. Phys. Soc. Japan* **43**, 907 (1977).
  - <sup>27</sup> F. J. Ohkawa and Y. Uemura, *J. Phys. Soc. Japan* **43**, 917 (1977).
  - <sup>28</sup> F. J. Ohkawa, *Solid State Commun.* **26**, 69 (1978).
  - <sup>29</sup> L. J. Sham and M. Nakayama, *Phys. Rev. B* **20**, 734 (1979).
  - <sup>30</sup> F. J. Ohkawa, *J. Phys. Soc. Japan* **46**, 736 (1979).
  - <sup>31</sup> T. Ando, *Phys. Rev. B* **19**, 3089 (1979).
  - <sup>32</sup> J. H. Davies, *The Physics of Low-Dimensional Semiconductors* (Cambridge Press, Cambridge, 1998).
  - <sup>33</sup> F. Long, W. E. Hagston, and P. Harrison, in *23rd International Conference on the Physics of Semiconductors*, edited by M. Sheffler and R. Zimmermann (World Scientific, Singapore, 1996) p. 819.
  - <sup>34</sup> C. Herring and E. Vogt, *Phys. Rev.* **101**, 944 (1956).
  - <sup>35</sup> F. Schäffler, *Semicond. Sci. Technol.* **12**, 1515 (1997).
  - <sup>36</sup> B. Koiller, X. Hu, and S. Das Sarma, *Phys. Rev. B* **66**, 115201 (2002).
  - <sup>37</sup> H. Fritzsche, *Phys. Rev.* **125**, 1560 (1962).
  - <sup>38</sup> W. D. Twose, in the Appendix of Ref. [37].
  - <sup>39</sup> B. A. Foreman, *Phys. Rev. B* **72**, 165345 (2005).
  - <sup>40</sup> K. Shindo and H. Nara, *J. Phys. Soc. Japan* **40**, 1640 (1976).
  - <sup>41</sup> X. Hu, B. Koiler, and S. Das Sarma, *Phys. Rev. B* **71**, 235332 (2005).
  - <sup>42</sup> C. J. Wellard, L. C. L. Hollenberg, F. Parisoli, L. M. Kettle, H.-S. Goan, J. A. L. McIntosh, and D. N. Jamieson, *Phys. Rev. B* **68**, 195209 (2003).
  - <sup>43</sup> C. J. Wellard and L. C. L. Hollenberg, *Phys. Rev. B* **72**,

- 085202 (2005).
- <sup>44</sup> L. C. L. Hollenberg, C. J. Wellard, and A. D. Greentree, unpublished.
- <sup>45</sup> P. von Allmen, private communication.
- <sup>46</sup> M. Nakayama and L. J. Sham, *Solid State Commun.* **28**, 393 (1978).
- <sup>47</sup> K. Takashina, Y. Ono, A. Fujiwara, Y. Takahashi, and Y. Hirayama, *Phys. Rev. Lett.* **96**, 236801 (2006).
- <sup>48</sup> M. M. Roberts, L. J. Klein, D. E. Savage, K. A. Slinker, M. Friesen, G. Celler, M. A. Eriksson, and M. G. Lagally, *Nature Mater.* **5**, 388 (2006).
- <sup>49</sup> M. Friesen, M. A. Eriksson, and S. N. Coppersmith, *Appl. Phys. Lett.* **89**, 202106 (2006).
- <sup>50</sup> M. Friesen and S. N. Coppersmith, unpublished.
- <sup>51</sup> *Handbook of Mathematical Functions*, edited by M. Abramowitz and I. A. Stegun (Dover, New York, 1972), Chap. 22.
- <sup>52</sup> S. Lee and P. von Allmen, cond-mat/0607462 (unpublished).
- <sup>53</sup> B. S. Swartzentruber, Y.-W. Mo, R. Kariotis, M. G. Lagally, and M. B. Webb, *Phys. Rev. Lett.* **65**, 1913 (1990).
- <sup>54</sup> N. G. Kharche, M. E. Prada, and G. Klimeck, unpublished.
- <sup>55</sup> M. O. Nestoklon, L. E. Golub, and E.L. Ivchenko, *Phys. Rev. B* **73**, 235334 (2006)